Original Article

JCBFM

Journal of Cerebral Blood Flow & Metabolism
2017, Vol. 37(6) 2171–2184

DOI: 10.1177/0271678X16662041
journals.sagepub.com/home/jcbfm
SAGE

K_{IR} channels tune electrical communication in cerebral arteries

Maria Sancho[1,2], Nina C Samson[2], Bjorn O Hald[3], Ahmed M Hashad[2], Sean P Marrelli[4], Suzanne E Brett[1,2] and Donald G Welsh[1,2]

Abstract

The conducted vasomotor response reflects electrical communication in the arterial wall and the distance signals spread is regulated by three factors including resident ion channels. This study defined the role of inward-rectifying K^+ channels (K_{IR}) in governing electrical communication along hamster cerebral arteries. Focal KCl application induced a vasoconstriction that conducted robustly, indicative of electrical communication among cells. Inhibiting dominant K^+ conductances had no attenuating effect, the exception being Ba^{2+} blockade of K_{IR}. Electrophysiology and Q-PCR analysis of smooth muscle cells revealed a Ba^{2+}-sensitive K_{IR} current comprised of $K_{IR}2.1/2.2$ subunits. This current was surprisingly small and when incorporated into a model, failed to account for the observed changes in conduction. We theorized a second population of K_{IR} channels exist and consistent with this idea, a robust Ba^{2+}-sensitive $K_{IR}2.1/2.2$ current was observed in endothelial cells. When both K_{IR} currents were incorporated into, and then inhibited in our model, conduction decay was substantive, aligning with experiments. Enhanced decay was ascribed to the rightward shift in membrane potential and the increased feedback arising from voltage-dependent-K^+ channels. In summary, this study shows that two K_{IR} populations work collaboratively to govern electrical communication and the spread of vasomotor responses along cerebral arteries.

Keywords

Electrophysiology, endothelium, microcirculation, potassium channels, smooth muscle

Received 11 March 2016; Revised 29 June 2016; Accepted 1 July 2016

Introduction

Cerebral resistance arteries, linked in series and parallel, form an integrated vascular network.[1,2] To match blood flow with neural activity, this arterial network must respond as a coordinated unit to stimuli, sparsely generated in the cortex.[3,4] Coordination among vascular segments and cells optimizes nutrient transport and its loss results in tissue hypoxia and diminished brain function.[2,3] Integrating the behavior of thousands of vascular cells requires the expression of gap junctions among smooth muscle cells, among endothelial cells and the two cell layers. These intercellular pores allow charge generated by ion channel activity to pass among neighboring cells, facilitating the synchronization of membrane potential, cytosolic [Ca^{2+}], and myosin light chain phosphorylation.[5] The structural design of gap junctions consists of two docking hemichannels, each of which contains six connexin (Cx) subunits, the dominant subtypes in vascular tissue being Cx37, Cx40, Cx43, and Cx45.[6,7]

Cell-to-cell communication is characteristically assessed in vascular tissue by discretely applying agents to a small portion of an intact resistance artery

[1]Department of Physiology and Pharmacology, University of Western Ontario, London, Canada
[2]Department of Physiology and Pharmacology, Hotchkiss Brain Institute, Libin Cardiovascular Institute, University of Calgary, Calgary, Canada
[3]Department of Biomedical Sciences, University of Copenhagen, Copenhagen, Denmark
[4]Department of Anesthesiology, Baylor College of Medicine, Houston, USA

Corresponding author:
Maria Sancho, Western Ontario University, 1151 Richmond Street North, London, Ontario N6A 5C1, Canada.
Email: mariasanchogonzalez@hotmail.com

in situ or in vitro.[3,8,9] This discrete application induces a localized change in membrane potential (V_M) due to the activation of resident ion channels. This response consequently spreads along endothelial cells via robust homologous gap junctions[10–12] and then radially to the smooth muscle layer via high resistance myoendothelial gap junctions.[13] This so-called conducted response is intriguing in that it is neither a passive or regenerative event. The extent to which it spreads is governed by two key factors including: (1) the relative expression of gap junctions among neighboring vascular cells; and (2) the intrinsic properties of resident ion channels.[14]

Resting V_M in vascular smooth muscle is determined by a dynamic interplay between depolarizing inward currents (Cl^- and nonselective cation channels), and hyperpolarizing outward currents, the latter of which includes voltage-gated (Kv), Ca^{2+}-activated (BK_{Ca}), ATP-sensitive (K_{ATP}), and inward-rectifying (K_{IR}) K^+ channels.[15–17] Careful consideration of biophysical properties indicates that Ba^{2+}-sensitive K_{IR} channels, tetramers of K_{IR} 2.1 and 2.2 subunits, could modulate the spread of electrical responses (Supplemental Figure 1).[18] Of particular note with this conductance is the small outward (hyperpolarizing) component, with its aptly named property of "negative slope conductance." This property ensures that channel activity will paradoxically increase with hyperpolarization and it is this aspect that could facilitate the longitudinal spread of dilation along an artery. While supportive observations have been provided,[18] studies have curiously overlooked its bidirectionality and the potential of K_{IR} to impact on the spread of depolarization/constriction. Indeed, if blocked, this conductance could attenuate the conducted depolarization/constriction by placing arteries in a depolarized state whereby voltage-dependent feedback from Kv and BK_{Ca} channels is enhanced.[19,20]

This study explored the role of K_{IR} channels in governing electrical communication and the spread of depolarizing/constricting responses in the cerebral circulation. Using a conduction protocol, we show that K_{IR} is unique from other K^+ conductances, as its inhibition attenuates focal depolarization from conducting along hamster middle cerebral arteries. A small Ba^{2+}-sensitive K_{IR} current was subsequently isolated in smooth muscle but when incorporated into a computer model, it failed to account for the changes in conduction decay observed in Ba^{2+}-treated arteries. We consequently searched for and found a second Ba^{2+}-sensitive K_{IR} current in endothelial cells comprised of $K_{IR}2.1/K_{IR}2.2$ subunits. When the second K_{IR} conductance was included into our computer model, simulated Ba^{2+} blockade (smooth muscle and endothelium) substantively attenuated electrical communication, as seen in our intact vessel experiments. In closing, our findings are the first to demonstrate that smooth muscle and endothelial cells each express a resident population of K_{IR} channels and both work cooperatively to modulate electrical communication in the cerebral circulation.

Material and methods

Animal procedures

All procedures were approved by the Animal Care Committees at the University of Calgary and the University of Western Ontario and complied with the Canadian Council on Animal Care and the ARRIVE (Animal Research: Reporting In Vivo Experiments) guidelines. Briefly, male golden Syrian hamsters (10–12 weeks of age, Charles River Canada) were euthanized via carbon dioxide asphyxiation. The brain was carefully removed and placed in ice-cold phosphate-buffered (pH 7.4) saline solution containing (mM) 138 NaCl, 3 KCl, 10 Na_2HPO_4, 2 NaH_2PO_4, 5 glucose, 0.1 $CaCl_2$, and 0.1 $MgSO_4$. Third-order middle cerebral arteries were carefully dissected out of surrounding tissue and cut into 2 mm segments.

Vessel myography

Middle cerebral artery segments were cannulated in a customized arteriograph and superfused with warm (37°C) physiological salt solution (PSS; pH 7.4) containing (mM) 119 NaCl, 4.7 KCl, 1.7 KH_2PO_4, 1.2 $MgSO_4$, 1.6 $CaCl_2$, 10 glucose, and 20 $NaHCO_3$. Arteries were equilibrated for 30 min at 15 mmHg intravascular pressure and contractile responsiveness assessed by brief (~10 s) exposure to 55 mM KCl. Following equilibration, intravascular pressure was slowly raised from 15 to 50 mmHg (in vivo pressure). Cerebral arteries were then exposed to bradykinin (15 μM) to confirm the presence of intact endothelium. Contractile responsiveness and minimum diameter were obtained by briefly superfusing arteries with 60 mM KCl; maximal diameter was obtained after each paired experiment by superfusing with a Ca^{2+}-free PSS containing 2 mM EGTA. Arterial diameter was monitored by using a 10X objective and an automated edge detection system (IonOptix, USA).

Conduction protocol

For all functional experiments, a standard conduction assay was utilized.[21] Briefly, a glass micropipette was placed near the end of the vessel and KCl pressure ejected (250 mM, 20 psi, 20 s pulse) onto a small portion of the arterial wall. The stimulus duration elicited a focal vasoconstrictor response of ~25 μm; this

represented ~50% of the maximal vasoconstrictor capacity (determined by superfusing arteries with 60 mM KCl) and within this functional range, changes in voltage should translate into a graded vasomotor response.[21] Arterial diameter was then monitored at 0, 450, 900, 1350, and 1800 μm distal to the site of stimulation. Superfusate and luminal flow ran in the opposite direction of conduction, ensuring that the conducted response was not the result of diffusion/convection (Figure 1, top diagram). This experiment was performed prior to and following the addition of a BK_{Ca} (Paxilline, 10 μM; $n=7$ arteries/group), Kv (4-AP, 100 μM; $n=7$ arteries/group), K_{ATP} (Glibenclamide, 30 μM; $n=7$ arteries/group), or K_{IR} ($BaCl_2$, 40 μM; $n=8$ arteries/group) channel inhibitors. Conduction decay, a functional assessment of communication efficiency is calculated as the change in diameter (between the 450 and 1800 μm sites) per 100 μm length of artery. Multiple K^+ channel inhibitors were not simultaneously applied due to potentially large shifts in baseline tone. In a state where the linear relationship between voltage, cytosolic Ca^{2+}, and diameter may not be maintained, the validity of the conduction assay as an arbiter of electrical communication would be questionable.

Isolation of arterial smooth muscle and endothelial cells

Smooth muscle cells from middle cerebral arteries were enzymatically isolated as previously described.[22] Briefly, arterial segments were placed in an isolation medium (37°C, 10 min) containing (in mM) 60 NaCl, 80 Na^+ glutamate, 5 KCl, 2 $MgCl_2$, 10 glucose, and 10 HEPES with 1 mg ml^{-1} BSA (pH 7.4). Vessels were then exposed to a two-step digestion process that involved (1) 12–15 min incubation in isolation media (37°C) containing 0.5 mg ml^{-1} papain and 1.5 mg ml^{-1} dithioerythritol; and (2) 10 min incubation in isolation medium containing 100 μM Ca^{2+}, 0.7 mg ml^{-1} type-F collagenase, and 0.4 mg ml^{-1} type-H collagenase. Following treatment, tissues were washed repeatedly with ice-cold isolation medium and titurated with a fire-polished pipette. Isolated smooth muscle cells were identified by their characteristic spindle-like shape and contractile behavior. Liberated cells were stored in ice-cold isolation medium for use the same day within ~6 h postdigestion.

For endothelial cell isolation, arterial segments were placed in an isolation medium (37°C, 10 min) containing (in mM) 140 NaCl, 5.5 KCl, 1 $MgCl_2$, 1.2 NaH_2PO_4, 5 glucose, 2 Na^+ pyruvate, 0.02 EDTA, and 10 HEPES with 0.1 mg ml^{-1} BSA (pH 7.3). Vessels were then exposed to a two-step digestion process that involved the following: (1) 30 min incubation in isolation media (37°C) containing 1 mg ml^{-1} BSA, 100 μM Ca^{2+}, 1 mg ml^{-1} papain, and 1 mg ml^{-1} dithioerythritol; and (2) 7–8 min incubation in isolation medium containing 1 mg ml^{-1} BSA, 100 μM Ca^{2+}, 0.9 mg ml^{-1} type-F collagenase, 0.6 mg ml^{-1} type-H collagenase, 5 mg ml^{-1} elastase, and 1 mg ml^{-1} trypsin inhibitor. Tissues were then washed repeatedly with ice-cold isolation medium and gently titurated with a fire-polished pipette. This isolation procedure yielded small groups of endothelial cells ECs (2–3 cells) and they were clearly identifiable by their rough shape and lack of voltage-dependent K^+ conductances. Isolated cells were stored in ice-cold isolation medium and used the same day for up to 4 h postdigestion.

Patch clamp electrophysiology

Conventional patch-clamp electrophysiology was used to measure whole-cell currents in both isolated smooth muscle (n = 7 cells/group) and endothelial cells (n = 7 cells/group). Briefly, recording electrodes (resistance of 5–8 MΩ when filled with solution) were pulled from borosilicate glass microcapillary tubes (Sutter Instruments, Novato, CA, USA), covered in dental wax to reduce capacitance, and backfilled with pipette solution containing (in mM) 5 NaCl, 35 KCl, 100 K^+ gluconate, 1 $CaCl_2$, 0.5 $MgCl_2$, 10 HEPES, 10 EGTA, 2.5 Na_2-ATP, and 0.2 GTP (pH 7.2). To attain whole-cell configuration, a pipette was then gently lowered on to a cell and negative pressure applied to achieve a Giga-ohm seal and rupture the membrane. Cells were voltage clamped (holding membrane potential −60 mV) and equilibrated for at least 15 min in a bath solution containing (in mM) 135 NaCl, 5 KCl, 0.1 $MgCl_2$, 10 HEPES, 10 glucose, and 0.1 $CaCl_2$. Smooth muscle and endothelial cells were held at −60 mV. Whole-cell currents were recorded on an Axopatch 200B amplifier (Axon Instruments, Union City, CA, USA), filtered at 1 kHz, digitized at 5 kHz, and were stored in a computer for subsequent offline analysis with Clampfit 10.3 software. Cell capacitance ranged between 14 and 18 pF in smooth muscle cells and 4–8 pF in endothelial cells was measured with the cancelation circuity in the voltage-clamp amplifier. Cells that displayed a noticeable shift in capacitance (>0.3 pF) during experiments were excluded for analysis. A NaCl-agar salt bridge between the Ag–AgCl reference electrode and the bath solution was used to minimize offset potentials. All experiments were performed at room temperature (20–22°C).

To monitor the Ba^{2+}-sensitive K_{IR} current, [K^+] was elevated from 5 to 60 mM via equimolar replacement of NaCl by KCl. Voltage was then stepped to −100 mV for 100 ms and then ramped to +20 mV at a rate of 0.04 mV ms^{-1}. The currents from three trials

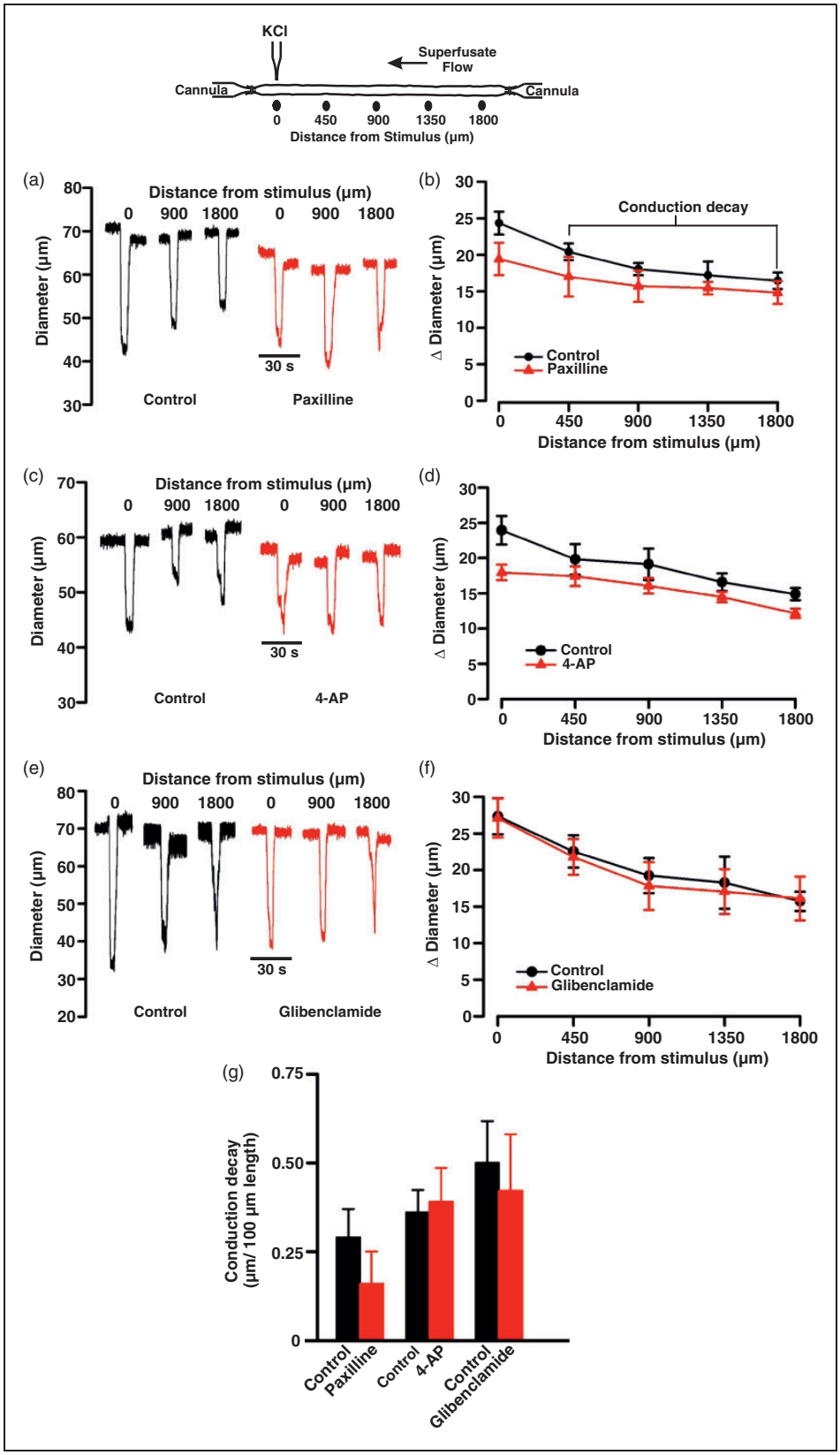

Figure 1. Modifying BK_{Ca}, Kv, and K_{ATP} channel activity does not affect conduction in cerebral arteries. Top: Illustration of the experimental protocol. KCl (250 mM, 20 s) was applied via pipette to the vessel wall while vasomotor responses are measured 0–1800 μm distal to the site of stimulation. Representative traces (a, c, and e) and summary plots (b, d, and f) highlight the inability

(continued)

(5 s between trails) were subsequently averaged. Ba^{2+} sensitivity was assessed by applying the preceding protocol to cells superfused with KCl 60 mM solution containing an increasing concentration (1 μM–1 mM) of this K_{IR} inhibitor for 2–3 min.

Q-PCR analysis of K_{IR} 2.x subtypes

Smooth muscle (~200) and endothelial cells (~100) were isolated from middle cerebral arteries (n = 4 arteries/group) and whole middle cerebral arteries (~2 from n = 4 arteries/group) and placed in RNase- and DNase-free collection tubes. Total RNA was extracted (RNeasy plus micro kit Qiagen, USA) and first-strand cDNA synthetized using the Quantitect reverse transcription kit (Qiagen) according to instructions. For the negative control groups, all components except the reverse transcriptase were included in the reaction mixtures. Q-PCR was performed using the Kapa SYBR Fast Universal qPCR Kit (Kapa Biosystems). Hamster beta actin (ACTB) gene was utilized as the reference gene. Control reactions and those containing cDNA from cerebral arteries were performed with 1 ng of template per reaction. Due to the very small quantities of RNA obtained from isolated smooth muscle cells (~200 cells), the entire cDNA yield from each preparation was used to assay the full set of test and housekeeping genes. The running protocol included 45 cycles consisting of 95°C for 5 s, 55°C for 15 s, and 72°C for 10 s using an Eppendorf Realplex 4 Mastercycler. PCR specificity was checked by dissociation curve analysis. Assay validation was confirmed by testing serial dilutions of pooled template cDNAs suggesting a linear dynamic range of 0.1–100 ng template and yielded percent efficiencies ranging from 85 to 108%. Template controls did not yield detectable fluorescence. Expression of the K_{IR}2.x isoforms in cerebral arteries, endothelial, or smooth muscle cells (n = 4 arteries/group) relative to control tissue was determined using the relative expression software tool (REST) version 2.0.13.[23]

The primers for RT-qPCR were as follows: K_{IR}2.1 (Accession XM_005069969) CCACTGGATCTTACA TGCTTCTG and AATGAGGAGAGATGGATGCT TCC; K_{IR}2.2 (Accession XM_005067657) CA GCATCGTGTCATCAGAGG and CGAACTCAAT GTTGCACTGG; K_{IR}2.3 (Accession XM_005066848) ATTGCAGTCGTGGTCCAGTC and GTCTGG GCCCTCTTCTT AGG; K_{IR}2.4 (Accession XM_ 005084695) CCCGCTAGGCCAAGTAGAG and CAGCTCGGCT GTCTCCTG; Actin (Accession NM_001281595) AGCACCCTGTGCTGCTCAC and GTACAT GGCTGGGGTGTTG.

Computational modeling

A computational model of a 2 mm length of cerebral artery (diameter, 40 μm) was developed from previous models of mesenteric arterioles.[24,25] The electrically sealed vessel segment comprised one layer of endothelial cells, each $100 \times 7.8 \times 1$ $(\mu m)^3$ in size and oriented along the vessel axis, and one layer of smooth muscle cells, each $63 \times 6.25 \times 5$ $(\mu m)^3$ in size and oriented perpendicularly (Figure 4(a)). Myoendothelial coupling resistance was equivalent to 900 MΩ per smooth muscle cell, whereas homocellular gap junctional resistances between endothelial or between smooth muscle cells were equivalent to 3 and 90 MΩ, respectively.[26] The electrophysiological properties of each cell type were adapted by fitting maximal activity parameters of ion channels, pumps, and exchangers to whole-cell IV-curves from cerebral SMCs and ECs, respectively. Note, the voltage-dependent outward K^+ current (Kv) was treated as a composite of conductances comprised of Kv1, Kv2, Kv7, and TWIK-2 channels.[27–30] Significant K_{IR} activity was retained in both cell types and we assumed that K_{IR} was maximally active at −60 mV, reversed at −80 mV, and activity was roughly halved at −40 mV.[19]

In intact arteries, electrical communication is assessed by applying vasoactive agents[8,11] or by injecting current.[31] These stimuli create a voltage differential and produce current flow between stimulated and non-stimulated cells. In our model, we created a voltage differential by voltage clamping (20 mV positive to the resting V_M of −40 mV) a defined number of endothelial and smooth muscle cells belonging to the initial 62 μm segment of the virtual artery. Voltage responses were subsequently calculated along the length of the virtual artery. A complete description of the model can be found in the online supplement.

Chemical, drugs, and enzymes

Glibenclamide, $BaCl_2$, bradykinin, buffer reagents, collagenases (types F and H), dithioerythritol, paxilline,

Figure 1. Continued
of paxilline, 4-AP, and glibenclamide, respectively, to affect the conducted constrictor response elicited by KCl. In (a), (b), and (c) absolute diameter at rest, with paxilline (10 μM); 4-AP (100 μM), or glibenclamide (30 μM), respectively, at maximum and at minimum were as follows: (a) ($n = 7$), 69 ± 4, 61 ± 3, 41 ± 3, and 77 ± 4 μm; (b) ($n = 7$), 68 ± 3, 61 ± 3, 41 ± 3, and 77 ± 4 μm; (c) ($n = 7$), 71 ± 3, 70 ± 3, 40 ± 3, and 87 ± 4 μm. Conduction decay constants (g, μm/100 μm) were as follows: control 0.29 ± 0.08, with paxilline 0.16 ± 0.09; control 0.36 ± 0.06, with 4-AP 0.39 ± 0.09 and control 0.50 ± 0.11, with glibenclamide 0.42 ± 0.15. Data are means ± SE.

trypsin inhibitor, and 4-AP were purchased from Sigma-Aldrich. Papain and elastase were acquired from Worthington (USA) and Calbiochem (USA), respectively.

Statistical analysis

Data are expressed as means ± SE and *n* indicates the number of vessels or cells. No more than two experiments were performed on vessels or cells from a given animal. Power analysis confirmed that n = 6/group was sufficient to observe statistical significance in our vessel/cell-based experiments. Paired *t* tests were performed on vessels or cells to compare the effects of a given condition/treatment on arterial diameter or whole-cell current (Graphpad PRISM 4.0, San Diego, CA, USA; and Sigmaplot, SPSS). *P* values ≤ 0.05 were considered statistically significant; experimental design and data presentation are reported in compliance with ARRIVE guidelines.

Results

K^+ channels and the tuning of electrical communication

Electrical communication was assayed by applying KCl (250 mM) to a small portion of a cerebral artery while monitoring diameter responses along its length (Figure 1 top). As denoted in Figure 1(a), focal KCl application elicited a constrictor response that conducted robustly and with modest decay (0.41 ± 0.05 μm/100 μm vessel length). The addition of BK_{Ca} (paxilline, 10 μM), Kv (4-AP, 100 μM), and K_{ATP} (glibenclamide, 30 μM) channel inhibitors to the superfusate had no measurable effect on local or conducted responses, or to the calculation of conduction decay (Figure 1(a) to (g)). In striking contrast, Ba^{2+} (40 μM) inhibition of the inward-rectifying K^+ (K_{IR}) channel markedly attenuated the ability of KCl-induced constriction to robustly conducting along cerebral arteries (Figure 2). Calculation of conduction decay in the

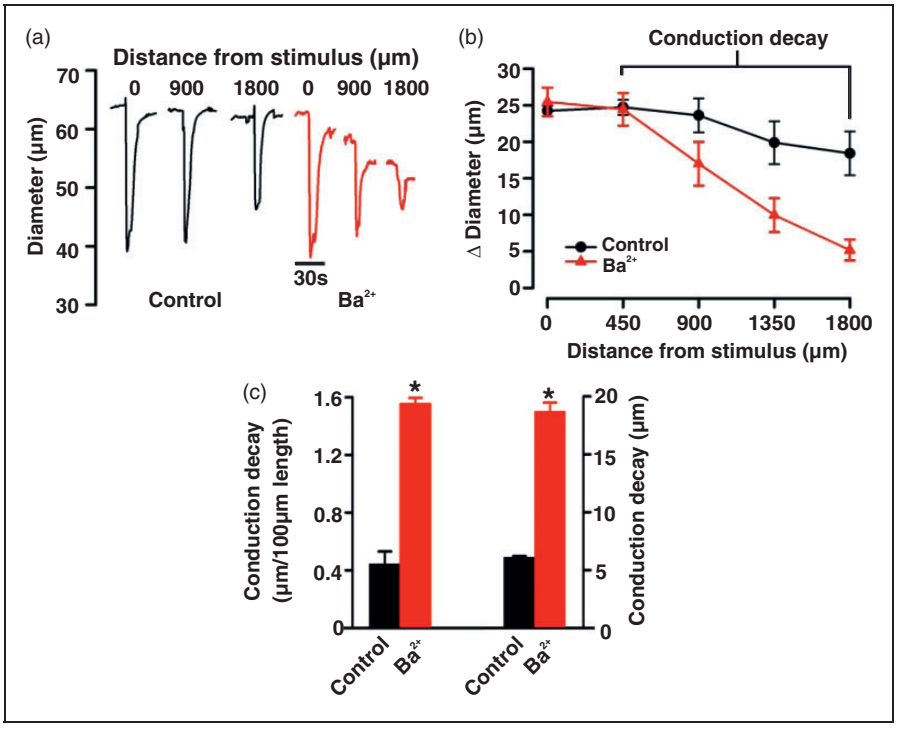

Figure 2. Ba^{2+} block of K_{IR} channels augments conduction decay. KCl (20 s) was focally applied to the vessel wall while diameter responses were monitored 0–1800 μm distal to the site of stimulation. Measurements were performed in the absence or presence of $BaCl_2$ (40 μM), a K_{IR} blocker. Representative trace (a) and summary plots (b and c) highlighting the effect of Ba^{2+} on peak constriction and conduction decay. In (b) ($n = 8$) absolute diameter at rest, with $BaCl_2$, at maximum and at minimum were as follows: 68 ± 2, 66 ± 2, 40 ± 2, and 77 ± 2 μm. In (c), conduction decay constants (μm/100 μm) and absolute conduction decay (μm) were as follows: control 0.44 ± 0.09, with Ba^{2+} 1.55 ± 0.04; control 6.10 ± 0.10, with Ba^{2+} 18.72 ± 0.74. Data are means ± SE. *Significant difference from control.

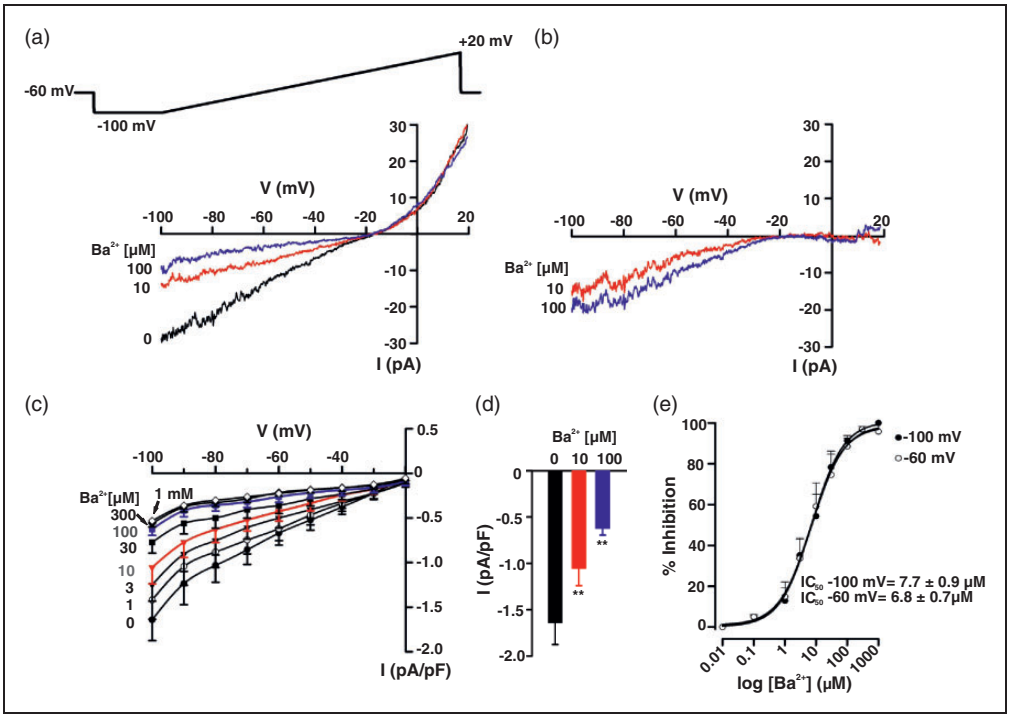

Figure 3. K_{IR} current in cerebral arterial smooth muscle cells. Whole-cell K^+ current was measured in isolated smooth muscle cells bathed in a high K^+ solution (60 mM) using a voltage ramp protocol (−100 to +20 mV) in presence and absence of $BaCl_2$ (1 μM–1 mM). Representative whole-cell current recording (a) and Ba^{2+}-subtracted currents (b). Summary plots ($n = 7$) illustrate the effect of Ba^{2+} (1 μM–1 mM) on whole-cell current (c) and on peak inward current at −100 mV (d). Ba^{2+} induces a concentration-dependent inhibition of K_{IR} current (e, $n = 7$) at both −100 mV ($IC_{50} = 7.70 \pm 0.85$ μM) and −60 mV ($IC_{50} = 6.78 \pm 0.67$ μM). Data are means ± SE. **Significant difference from control.

absence and the presence of Ba^{2+} were 0.45 ± 0.09 and 1.55 ± 0.04/100 μm vessel length, respectively ($P < 0.05$ (Figure 2(c))).

K_{IR} channel expression in cerebral arterial smooth muscle

Mindful of the preceding observations, patch-clamp electrophysiology was used to delineate K_{IR} channels in cerebral arterial smooth muscle cells. Basic procedures consisted of measuring whole current in cells bathed in 60 mM K^+ and a variable concentration of Ba^{2+} (1 μM–1 mM), a selective, concentration-dependent inhibitor of K_{IR}. Findings in Figure 3(a) denote that whole-cell current was divisible into a Ba^{2+}-sensitive and -insensitive component, with the former, inward at voltages negative to the K^+ equilibrium potential (E_K, −19.5 mV according to the Nernst equation). Barium subtracted currents in Figure 3(b) display characteristic inward-rectifying properties; mean data from seven SMCs (corrected for cell capacitance) are plotted in Figure 3(c) and (d). Calculations were performed in Figure 3(e) and they denote that Ba^{2+} inhibits K_{IR} in a concentration-dependent manner ($IC_{50} = 6.78 \pm 0.67$ μM, at −60 mV). K_{IR} currents in hamster cerebral arterial smooth muscle were appreciably smaller (-1.64 ± 0.23 pA/pF, at −100 mV) and exhibited lower sensitivity to Ba^{2+} compared to previous work performed in rat brain vessels.[32]

Computational modeling is an ideal tool to investigate how particular conductances influence the nature of electrical communication in the arterial wall. In this regard, we adapted an existing virtual model[24] to ascertain whether the subtraction of a K_{IR}-like current impacts upon the spread of depolarization, the signal driving conducted vasoconstriction. Akin to previous studies,[19] the K_{IR} current was assumed to be maximally active at −60 mV (~0.2 pA/pF), reversed at −80 mV, roughly halved at −40 mV, and retain the property of negative slope conductance. Figure 4 highlights that voltage clamping a defined number of vascular cells in the initial 62 μm segment of the virtual artery (20 mV positive to resting V_M) initiated a depolarization that conducted first along the endothelium and then radially to SMCs via myoendothelial gap junctions. Removing a K_{IR}-like current from the smooth muscle ionic

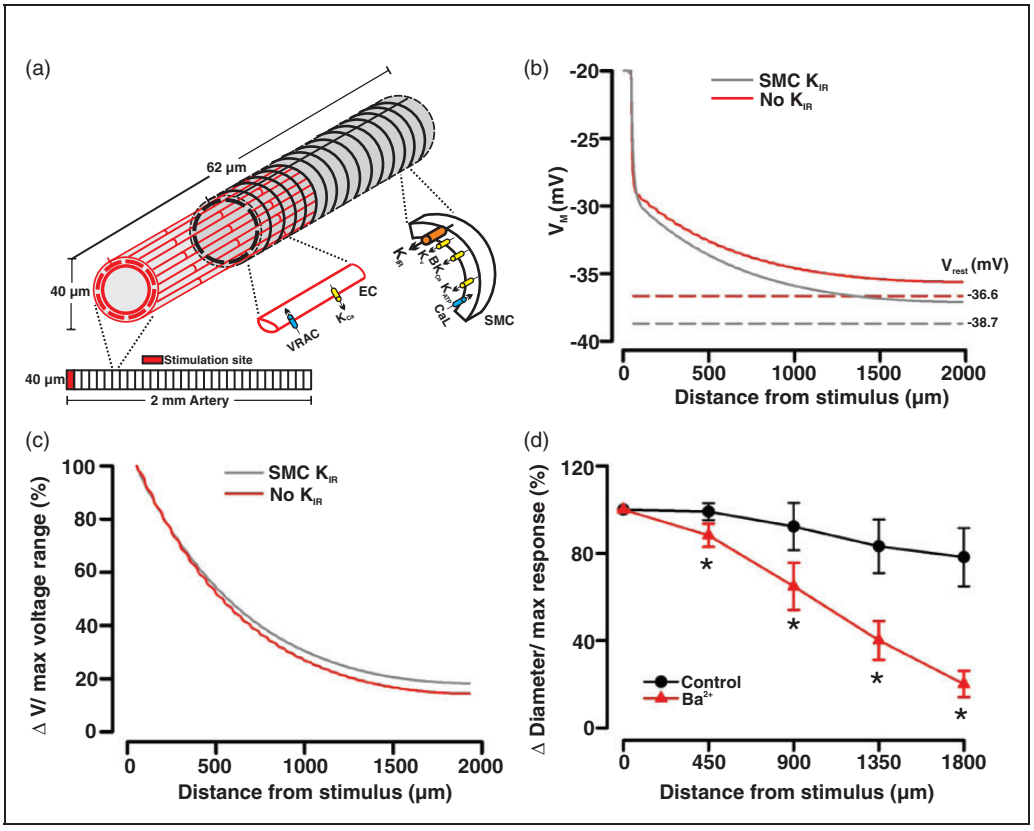

Figure 4. K_{IR} block in smooth muscle cells modestly attenuates electrical communication along the vessel length. General illustrative diagram (a) of the virtual artery. The virtual artery was 2.0 mm long and comprised one layer of endothelial cells ECs (red, light shaded) and one layer of smooth muscle cells (black, dark shaded). Endothelial cells were oriented lengthwise along the vessel, whereas smooth muscle cells ran perpendicularly. Within each layer, the cells form an overlapping pattern. Cells were treated as discrete elements with defined physical dimensions, gap junctional coupling, and ionic conductance. Simulation in (b): a defined number of endothelial and smooth muscle cells in the initial 62 µm segment of the virtual vessel were voltage clamped (200 ms) 20 mV positive to the resting V_M (−40 mV), while voltage responses were monitored at rest (SMC K_{IR}) and following the subtraction of a smooth muscle K_{IR} current (no K_{IR}). Dotted lines represent resting V_M (V_{rest}) under control conditions (gray, V_M: −38.7 mV) and following the subtraction of K_{IR} current in the smooth muscle layer (red, V_M: −36.6 mV). Conduction decay (c) along the virtual vessel under control conditions and in the absence of smooth muscle K_{IR} current. KCl was ejected onto a discrete region of a cerebral artery (d) while diameter responses (expressed relative to the maximal constrictor response, %) were monitored along the vessel length. Summary plot highlights the effect of Ba^{2+} (40 µM) on conducted vasomotor responses. Note, data in (d) originate from Figure 2(b) and has been reexpressed to facilitate comparisons with the computational observations.

representation shifted V_M rightward (−38.69 to −36.66 mV). Its impact on the spread of depolarization along the virtual artery was modest (Figure 4(b) and (c)) and did not align with the more dramatic Ba^{2+}-induced enhancement in vasomotor decay (Figure 4(d)). This disparate observation was suggestive of an additional pool of K_{IR} channels residing in the arterial wall.

K_{IR} channel expression in cerebral arterial endothelium

To consider whether an additional K_{IR} channel population is present in the cerebral circulation, Q-PCR was performed on whole arteries, smooth muscle, and endothelial cells, focusing on the four members of the $K_{IR}2.x$ subfamily.[32] Figure 5 summarizes the mRNA expression patterns and it denotes robust expression of $K_{IR}2.1/K_{IR}2.2$ in both cell types and the intact vessel, with K_{IR} 2.1 being the most abundant (~2–18-fold higher than K_{IR} 2.2). Previous studies have shown that K_{IR} currents comprised of $K_{IR}2.1/K_{IR}2.2$ will display higher Ba^{2+} sensitivity and the intrinsic property of negative slope conductance.[33] The latter ensures K_{IR} channel activity decreases with depolarization due to the voltage-dependent modulation of the Mg^{2+}/polyamine block.[15,34] This study found no consistent evidence of $K_{IR}2.3/K_{IR}2.4$ mRNA expression.

Patch-clamp electrophysiology was subsequently used to delineate K_{IR} channels in cerebral arterial endothelial cells. Basic procedures are outlined above and

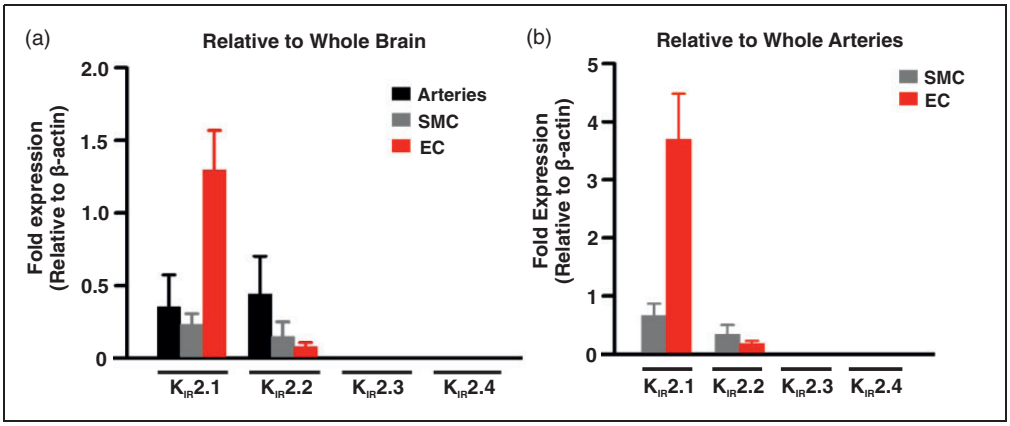

Figure 5. Q-PCR analysis of K_{IR} 2.x subtypes. mRNA expression (a) of K_{IR} 2.1–2.4 in whole middle cerebral arteries ($n = 4$), isolated smooth muscle ($n = 4$), and endothelial ($n = 4$) cells relative to whole brain mRNA expression. mRNA expression (b) of K_{IR} 2.1–2.4 in isolated SMCs ($n = 4$) and ECs ($n = 4$) cells relative to whole middle cerebral arteries mRNA expression. Data (means ± SE) are expressed relative to β-actin expression. Note that K_{IR} 2.3 and 2.4 mRNA was not detectable in selected tissues.

consisted of bathing endothelial cells in 60 mM K^+ solution and monitoring whole currents as the concentration of Ba^{2+} (1 μM–1 mM) was progressively increased. Endothelial whole-cell currents were divisible into a Ba^{2+}-sensitive and -insensitive component, the former being inward at voltages negative to the K^+ equilibrium potential (Figure 6(a), −19.5 mV). Barium subtracted currents clearly display inward-rectifying properties and mean data (corrected for cell capacitance) are summarized in Figure 6(b) to (d). Interestingly, endothelial K_{IR} currents were modestly more sensitive to Ba^{2+} ($IC_{50} = 0.67 \pm 0.02$ μM, at −60 mV) than those expressed in smooth muscle ($IC_{50} = 6.78 \pm 0.67$ μM, at −60 mV). The amplitude of the endothelial K_{IR} current was ~1.5-fold greater than smooth muscle (2.54 ± 0.33 pA/pF, at −100 mV) and this difference was conservatively incorporated into our computational model. As such, the endothelial K_{IR} current was assumed to be maximally active at −60 mV (~ 0.3 pA/pF), reversed at −80 mV, and roughly halved at −40 mV. Simulations were subsequently run to ascertain the spread of depolarization under control conditions and following the removal of both K_{IR} currents from our ionic representations. Figure 6(f) and (g) notes that the removal of the endothelial/smooth muscle K_{IR} currents induced a rightward (depolarizing) shift in the current–voltage relationship and consequently the virtual artery depolarized from −41.5 to −36.7 mV. This sizable voltage shift enhanced conduction decay and these virtual observations better aligned with the functional findings in Figure 4(d).

Discussion

This study focused on the conducted vasomotor response and the role of K_{IR} channels play in setting the distance over which it spreads along cerebral arteries. Functional work first revealed that Ba^{2+}, a selective K_{IR} channel inhibitor uniquely attenuated the conduction of constriction whereas other K^+ channel inhibitors had no effect. Patch-clamp electrophysiology and Q-PCR confirmed that a Ba^{2+}-sensitive K_{IR} current was present in vascular smooth muscle and likely comprised of $K_{IR}2.1/2.2$ subunits. Computational modeling revealed that this current was insufficient to account for the dramatic Ba^{2+}-induced enhancement of conduction decay. We consequently isolated endothelial cells and found a second, more robust Ba^{2+}-sensitive K_{IR} current. The incorporation of this second conductance into our virtual model was impactful, as simulations noted enhanced and substantive conduction decay after both K_{IR} currents (smooth muscle and endothelial) were eliminated from our ionic representations. From these findings, we conclude that there are two distinct pools of K_{IR} channels and that they collaboratively govern electrical communication and the ability of vasomotor responses to spread along and between cerebral arteries.

Background and findings

Cerebral arterial networks are comprised of hundreds of vessel segments, each of which responds to stimuli discretely and heterogeneously generated in brain tissue. These stimuli produce spatially unique vasomotor responses that tune blood flow delivery with energetic demand.[3,4] To maximize blood flow down a given arteriole, it is essential for multiple arterial segments and thousands of composite cells to respond as an integrated unit. Coordinating the behavior of vascular cells requires the spread of a common signal, like electrical charge, via gap junctions.[9] As charge passes

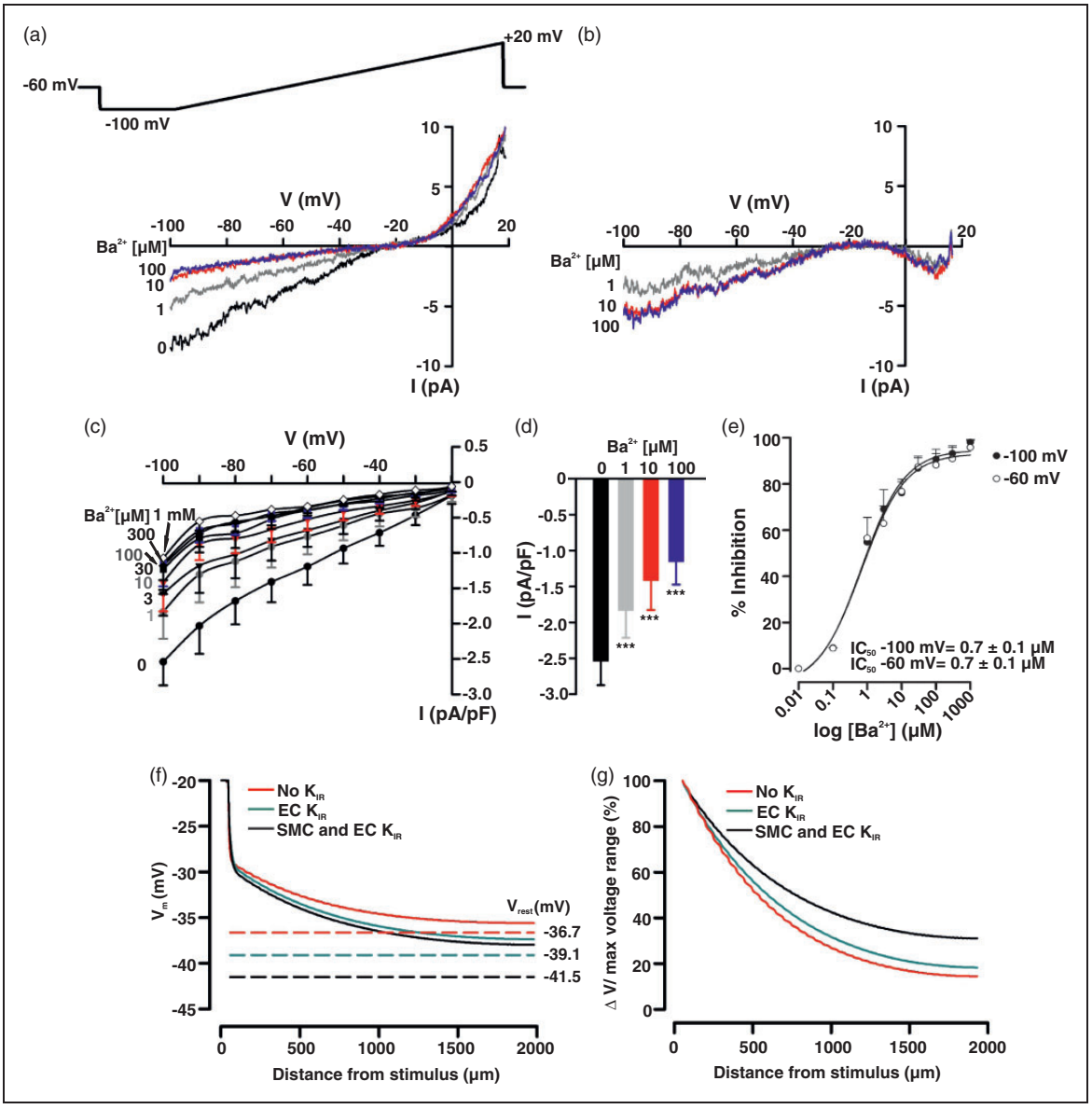

Figure 6. K_{IR} current in cerebral arterial endothelial cells and its virtual impact on conducted depolarization. Whole-cell K^+ current was measured in isolated endothelial cells in a high K^+ solution (60 mM) using a voltage ramp protocol (−100 to +20 mV) in presence and absence of $BaCl_2$ (1 μM–1 mM). Representative whole-cell current recording (a) and Ba^{2+}-subtracted currents (b). Summary plots ($n = 7$) illustrating the effect of Ba^{2+} (1 μM–1 mM) on whole-cell current (c) and on peak inward current at −100 mV (d). Ba^{2+} induces a concentration-dependent inhibition of K_{IR} current (E, $n = 7$) at −100 mV ($IC_{50} = 0.68 \pm 0.02$ μM) and −60 mV ($IC_{50} = 0.67 \pm 0.02$ μM). Data are means ± SE. **Significant difference from control. Simulation in (f): a defined number of endothelial and smooth muscle cells in the initial 62 μm segment of the virtual vessel (see Figure 4 for details) were voltage clamped (200 ms) 20 mV positive to the resting V_M (−40 mV), while voltage responses were monitored at rest (smooth muscle and endothelial K_{IR}) and following the subtraction of K_{IR} current in one or both cell types. Dotted lines represent resting V_M (V_{rest}) under control conditions (black, V_M: −38.7 mV), and following the subtraction of K_{IR} conductance in the endothelium (green, V_M: −39.1 mV) or both cell layers (red, V_M: −36.7 mV). Conduction decay (g) along the virtual vessel under control conditions and in the absence of one or both K_{IR} currents.

through these intercellular pores, arterial V_M balances among neighboring cells and this in turn guide aids in directing smooth muscle [Ca^{2+}] and myosin light chain phosphorylation.[5]

The conducted vasomotor response is the functional expression of organized cellular behavior in the arterial wall. This functional assay is typically initiated by focally applying agents to one end of an artery to trigger

a change in endothelial V_M. The generation of this focal electrical response enables charge movement first along the endothelium,[10–12] and then to overlying smooth muscle via myoendothelial gap junctions.[13] As smooth muscle V_M changes, so does the activity of L-type Ca^{2+} channels, the primary driver of cytosolic [Ca^{2+}]. The distance over which electrical phenomena spreads is governed by two key elements which include gap junctional resistivity and the properties of active ion channels.[14] While a variety of ionic conductances set resting V_M and basal tone,[15–17] K_{IR} channels appear ideally suited to modulate charge spread along the arterial wall due to negative slope conductance. This intrinsic property enables K_{IR} activity to passively increase with hyperpolarization and thus facilitate the conduction of vasodilatory response.[15,34] Overlooked in past examinations is the potential bidirectionality of K_{IR} and its impact on the spread of depolarizing/constrictor responses due to its ability to shift arterial V_M and alter negative feedback from Kv or BK_{Ca} channels.

To test this novel yet fundamental concept in the cerebral circulation, we began pulsing KCl onto isolated middle cerebral arteries to elicit a localized depolarization. We observed for the first time a vasoconstriction that conducted robustly to four distal sites along the arterial wall. Akin to previous studies,[18] we calculated conduction decay to functionally assess charge loss along the vascular structure; control values typically ranged between 0.4 and 0.5 μm/100 μm vessel length. We subsequently observed that selective inhibition of BK_{Ca}, Kv, and K_{ATP} channel failed to attenuate the spreading response or impact conduction decay (Figure 1). In striking contrast, Ba^{2+} block of K_{IR} dramatically affect both parameters (Figure 2), a finding which highlights that ion channels, with presumably appropriate biophysical properties, can impact conduction. As noted previously, we conceptually ascribed the ability of K_{IR} blockade to attenuate conducted constriction to two interrelated effects. First, micromolar Ba^{2+} reduces negative slope conductance, a unique K_{IR} property that places a tonic hyperpolarizing effect on the arterial wall.[18,32] Eliminating this property will induce a rightward (depolarizing) shift in arterial V_M, placing arteries in a state where a spreading KCl-induced depolarization will be countered by greater Kv/BK_{Ca} channel activity.[19,20]

Having defined a key role for K_{IR} in facilitating the conducted constriction, we next determined the cell type in which K_{IR} channels are expressed. Respectful of past observations,[18,19,32] initial efforts focused on vascular smooth muscle where patch clamp electrophysiology confirmed the presence of a Ba^{2+}-sensitive K_{IR} current (Figure 3). Compared to rat, whole-cell currents in hamster cerebral arterial smooth muscle cells were modestly more sensitive to Ba^{2+} although decidedly smaller.[19,32] This latter observation raises an important question, "Is this current sufficient to account for the functional phenotype." We consequently adapted a computational model[24,25] and ran simulations whereby electrical conduction was monitored under control conditions and following the subtraction of a K_{IR}-like current from the smooth muscle representation. This virtual work revealed that while V_M shifted rightward following the removal of the K_{IR}-like current, the change in conduction was limited. These results might suggest that Ba^{2+} is less selective than initially thought although this scenario appears unlikely.[15,35,36] A second, more exciting possibility is the presence of an additional population of K_{IR} channels in the arterial wall which has yet to be identified.

With due consideration of the second possibility, we considered whether an unexpected population of K_{IR} channels was present in the endothelial cells. Consistent with this prospect, real-time PCR analysis revealed that $K_{IR}2.1$/$K_{IR}2.2$ mRNA expression was not limited to cerebral arterial smooth muscle but extended to the endothelium (Figure 5). Whole-cell patch clamp electrophysiology subsequently confirmed a robust Ba^{2+}-sensitive K_{IR} current in freshly isolated endothelial cells whose current density and sensitive to Ba^{2+} was greater than smooth muscle (Figure 6). The latter finding suggests that endothelial K_{IR} channels may contain more $K_{IR}2.2$ subunits than smooth muscle.[37] When both currents were incorporated into and then blocked in our computational model, we observed a markedly greater attenuation of conduction (Figure 6(f) and (g)), findings that better aligned with our experimental observations. The idea that endothelial K_{IR} channels have a sizable impact on vascular function is supported by Sonkusare et al. who recently showed in mesenteric arteries that this conductance not only mediated K^+-induced vasodilation but appeared to "boost" the ability of other endothelial K^+ conductances to drive vessel relaxation.[38]

Broader implications

Arteries and capillaries in the cerebral circulation respond to sparsely generated stimuli eliciting coordinated multisegmental responses that tune blood flow delivery to brain function.[3,39] This behavior is extraordinary and one that reflects electrical responses conducting among and between endothelial and smooth muscle cells.[40,41] Electrical communication in the arterial wall is often viewed as a passive phenomenon with responses electronically decaying as they spread. Juxtapositioned to this idea, this study offers that new view that electrical communication in vascular tissue

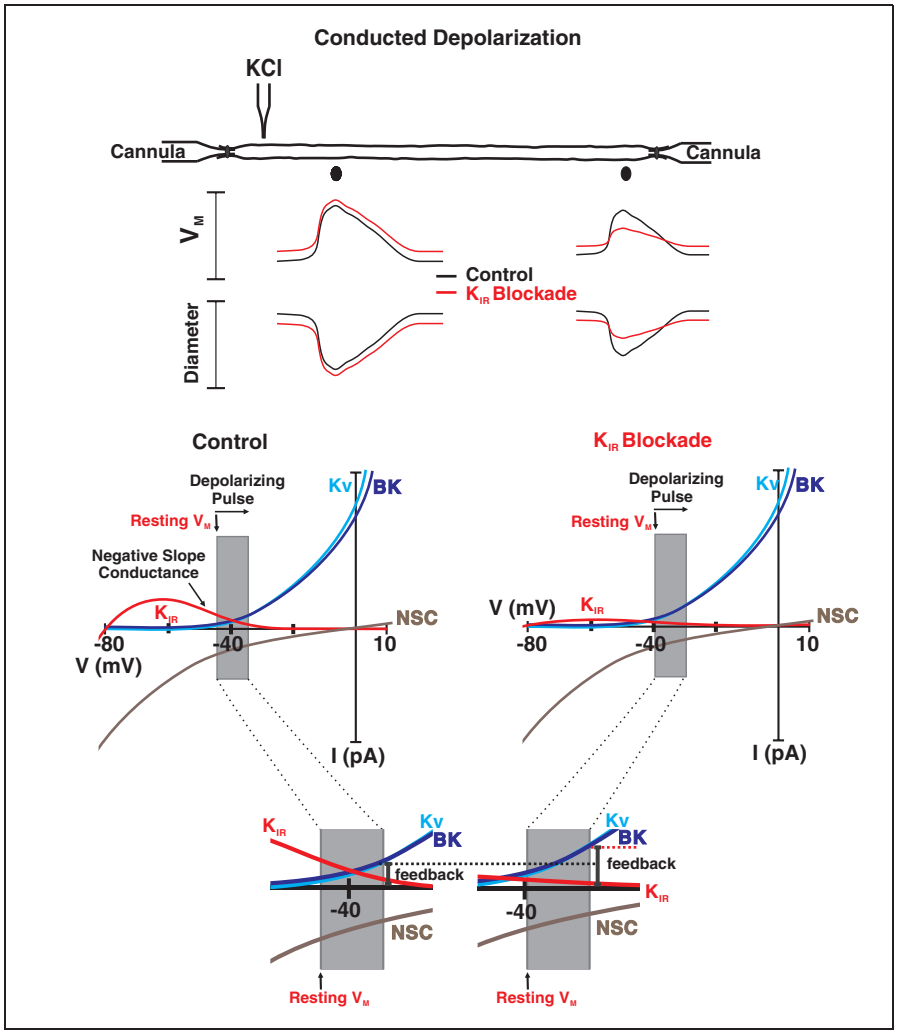

Figure 7. Stylized diagram of "pliancy" and the effect of K_{IR} blockade on conducted depolarization. Under control conditions, (resting V_M, −45 mV), a KCl-induced depolarization will reduce tonic K_{IR} activity while modestly increasing the activity of voltage-dependent (Kv) and large conductance Ca^{2+}-activated K^+ channels. Barium will attenuate conducted depolarization/constriction by first eliminating the unique K_{IR} property of negative slope conductance. This will place arteries in a more depolarized state such that when KCl is focally applied, the resulting conducted response will be more robustly countered by BK and Kv channel activity. This is best observed in the magnified inset. NSC denotes inward nonselective cation (NSC) currents.

is a "Pliant" process.[24,42] The concept of pliancy centers on the possibility of voltage-dependent ion channels modifying charge loss through the plasma membrane and thus the spread of electrical responses. In detail, we propose (see Figure 7) that K_{IR} channels modulate conducted constriction by shifting resting V_M such that spreading depolarization encounters a variable degree of negative feedback from K_V and BK channels. Linking K_{IR} to the concept of "pliancy" has intriguing implications to how the field views of cerebral vascular dysfunction. A reduction in this key ion channel conductance, as can occur in hypertension or prolonged stress, will not only enhance basal tone but impair the coordination of the arterial segments needed to properly match blood flow delivery with local metabolic demand.[43–45] Arguably, physiological stimuli that reduce phosphatidylinositol 4,5 bisphosphate, a key regulator of $K_{IR}2.x$ channels would also impact the conducted response and the nature of blood flow control.[46]

Summary

This study provided evidence that inwardly rectifying Ba^{2+}-sensitive channels comprised of $K_{IR}2.1/2.2$ subunits are present in both endothelial and smooth muscle cells of the hamster cerebral arteries. Endothelial K_{IR} channels and those in smooth muscle facilitate electrical communication by limiting the extent to which a conducted response decays along

the arterial wall. These observations provide new insights into how distinct populations of the same ion channel work cooperatively to shape charge movement and consequently the multisegmental responses need to blood flow delivery with local metabolic demand.

Funding

The author(s) disclosed receipt of the following financial support for the research, authorship, and/or publication of this article: This research was supported by an operating grant from the Canadian Institute of Health Research. DG Welsh is Rorabeck Chair of Molecular Neuroscience and Vascular Biology at the University of Western Ontario. AM Hashad was supported by a Vanier scholarship and an AI-HS graduate studentship. SPM was supported by grants from the National Institute of Health (R21NS090129, and R56NS096186).

Declaration of conflicting interests

The author(s) declared no potential conflicts of interest with respect to the research, authorship, and/or publication of this article.

Authors' contribution

All the authors have made substantial contribution to the manuscript: DGW and MS conceived and designed the research, drafted the manuscript, and made critical revisions. MS, NCS, BOH, AMH, SM, and SEB acquired, analyzed, and interpreted the data, and made critical revisions to the manuscript.

Supplementary material

Supplementary material for this paper can be found at http://jcbfm.sagepub.com/content/by/supplemental-data

References

1. Faraci FM and Heistad DD. Regulation of cerebral blood vessels by humoral and endothelium-dependent mechanisms. Update on humoral regulation of vascular tone. *Hypertension* 1991; 17: 917–922.
2. Faraci FM and Heistad DD. Regulation of the cerebral circulation: role of endothelium and potassium channels. *Physiol Rev* 1998; 78: 53–97.
3. Segal SS and Duling BR. Flow control among microvessels coordinated by intercellular conduction. *Science* 1986; 234: 868–870.
4. Segal SS and Jacobs TL. Role for endothelial cell conduction in ascending vasodilation and exercise hyperanemia in hamster skeletal muscle. *J Physiol* 2001; 536: 937–946.
5. Figueroa XF, Isakson BE and Duling BR. Connexins: gaps in our knowledge of vascular function. *Physiology (Bethesda)* 2004; 19: 277–284.
6. Gustafsson F, Mikkelsen HB, Arensback B, et al. Expression of connexion 37, 40 and 43 in rat mesenteric arterioles and resistance arteries. *Histochem Cell Biol* 2003; 119: 139–148.
7. Li X and Simard JM. Connexin45 gap junction channels in rat cerebral vascular smooth muscle cells. *Am J Physiol Heart Circ Physiol* 2001; 281: H1890–H1898.
8. Welsh DG and Segal SS. Endothelial and smooth muscle cell conduction in arterioles controlling blood flow. *Am J Physiol Heart Circ Physiol* 1998; 274: H178–H186.
9. Segal SS, Welsh DG and Kurjiaka DT. Spread of vasodilation and vasoconstriction along feed arteries and arterioles of hamster skeletal muscle. *J Physiol* 1999; 516: 283–291.
10. Emerson GG and Segal SS. Electrical coupling between endothelial cells and smooth muscle cells in hamster feed arteries: role in vasomotor control. *Circ Res* 2000; 87: 474–479.
11. Emerson GG and Segal SS. Endothelial cell pathway for conduction of hyperpolarization and vasodilation along hamster feed artery. *Circ Res* 2000; 86: 94–100.
12. Takano H, Dora KA, Spitaler MM, et al. Spreading dilation in rat mesenteric arteries associated with calcium in dependent endothelial cell hyperpolarization. *J Physiol* 2004; 556: 887–903.
13. Tran CH, Vigmond EJ, Goldman D, et al. Electrical communication in branching arterial networks. *Am J Physiol Heart Circ Physiol* 2012; 303: H680–H692.
14. Nielsen MS, Axelsen LN, Sorgen PL, et al. Gap Junctions. *Compr Physiol* 2012; 2: 1981–2035.
15. Nelson MT and Quayle JM. Physiological roles and properties of potassium channels in arterial smooth muscle. *Am J Physiol* 1995; 268: C799–C822.
16. Quayle JM, Nelson MT, Standen NB, et al. ATP-sensitive and inwardly rectifying potassium channels in smooth muscle. *Physiol Rev* 1997; 77: 1165–1232.
17. Jackson WF. Potassium channels in the peripheral microcirculation. *Microcirculation* 2005; 12: 113–127.
18. Jantzi MC, Brett SE, Jackson WF, et al. Inward rectifying potassium channels facilitate cell-to-cell communication in hamster retractor muscle feed arteries. *Am J Physiol Heart Circ Physiol* 2006; 291: H1319–H1328.
19. Wu BN, Luykenaar KD, Brayden JE, et al. Hypoosmotic challenge inhibits inward rectifier K^+ channels in cerebral arterial smooth muscle cells. *Am J Physiol Heart Circ Physiol* 2007; 292: H1085–H1094.
20. Knot HJ, Zimmermann PA and Nelson MT. Extracellular K(+)-induced hyperpolarizations and dilations of rat coronary and cerebral arteries involve inward rectifier K (+) channels. *J Physiol* 1996; 492: 419–430.
21. Kurjiaka DT, Bender SB and Nye DD. Hypertension attenuates cell-to-cell communication in hamster retractor muscle feed arteries. *Am J Physiol Heart Circ Physiol* 2005; 288: H861–H870.
22. Anfinogenova Y, Brett SE, Walsh MP, et al. Do TRPC-like currents and G protein-coupled receptors interact to facilitate myogenic tone development? *Am J Physiol Heart Circ Physiol* 2011; 301: H1378–H1388.
23. Pfaffl MW, Horgan GW and Dempfle L. Relative expression software tool (REST) for group-wise comparison and statistical analysis of relative expression results in real-time PCR. *Nucleic Acids Res* 2002; 30: e36.

24. Hald BO, Jensen LJ, Sorensen PG, et al. Applicability of cable theory to vascular conducted responses. *Biophys J* 2012; 102: 1352–1362.
25. Kapela A, Nagaraja S and Tsoukias NM. A mathematical model of vasoreactivity in rat mesenteric arterioles. II. Conducted vasoreactivity. *Am J Physiol Heart Circ Physiol* 2010; 298: H52–H65.
26. Diep HK, Vigmond EJ, Segal SS, et al. Defining electrical communication in skeletal muscle resistance arteries: a computational approach. *J Physiol* 2005; 568: 267–281.
27. Knot HJ and Nelson MT. Regulation of membrane potential and diameter by voltage-dependent k+ channels in rabbit myogenic cerebral arteries. *Am J Physiol Heart Circ Physiol* 1995; 269: H348–H355.
28. Nelson MT and Quayle JM. Physiological roles and properties of potassium channels in arterial smooth muscle. *Am J Physiol Cell Physiol* 1997; 268: C799–C822.
29. Zhong XZ, Harhun MI, Olesen SP, et al. Participation of KCNQ (Kv7) potassium channels in myogenic control of cerebral arterial diameter. *J Physiol* 2010; 588: 3277–3293.
30. Bryan RM Jr, You J, Phillips SC, et al. Evidence for two-pore domain potassium channels in rat cerebral arteries. *Am J Physiol Heart Circ Physiol* 2006; 291: H770–H780.
31. Emerson GG, Neild TO and Segal SS. Conduction of hyperpolarization along hamster feed arteries: augmentation by acetylcholine. *Am J Physiol Heart Circ Physiol* 2002; 283: H102–H109.
32. Smith PD, Brett SE, Luykenaar KD, et al. KIR channels function as electrical amplifiers in rat vascular smooth muscle. *J Physiol* 2008; 586: 1147–1160.
33. Dhamoon AS, Pandit SV, Sarmast F, et al. Unique Kir2x properties determine regional and species differences in the cardiac inward rectifier K^+ current. *Circ Res* 2004; 94: 1332–1339.
34. Matsuda H, Oishi K and Omori K. Voltage-dependent gating and block by internal spermine of the murine inwardly rectifying K^+ cannel, Kir2.1. *J Physiol* 2003; 548: 361–371.
35. Nelson MT, Patlak JB, Worley JF, et al. Calcium channels, potassium channels, and voltage dependence of arterial smooth muscle tone. *Am J Physiol* 1990; 259: C3–C18.
36. Campanucci VA, Fearon IM and Nurse CA. A novel O2-sensing mechanism in rat glossopharyngeal neurones mediated by halothane-inhibitable background K+ conductance. *J Physiol* 2003; 548: 731–743.
37. Schram G, Pourrier M, Wang Z, et al. Barium block of Kir2 and human cardiac inward rectifier currents: evidence for subunit-heteromeric contribution to native currents. *Cardiovasc Res* 2003; 59: 328–338.
38. Sonkusare S, Dalsgaard T, Bonev A, et al. Inward rectifier potassium (Kir2.1) channels as end-stage boosters of endothelium-dependent vasodilators. *J Physiol* 2016; 594: 3271–3285.
39. Gaskell WH. The changes of the blood-stream in muscles through stimulation of their nerves. *J Anat Physiol* 1877; 11: 360–402.
40. Bagher P and Segal SS. Regulation of blood flow in the microcirculation: role of conducted vasodilation. *Acta Physiol (Oxf)* 2011; 202: 271–284.
41. Welsh DG and Taylor MS. Cell-cell communication in the resistance vasculature: the past, present, and future. *Microcirculation* 2012; 19: 377–378.
42. Hald BO, Jacobsen JC, Braunstein TH, et al. BKCa and KV channels limit conducted vasomotor responses in rat mesenteric terminal arterioles. *Plfugers Arch* 2012; 463: 279–295.
43. Goto K, Rummery NM, Grayson TH, et al. Attenuation of conducted vasodilation in rat mesenteric arteries during hypertension: role of inwardly rectifying potassium channels. *J Physiol* 2004; 561: 215–231.
44. Weston AH, Porter EL, Harno E, et al. Impairment of endothelial SK(Ca) channels and of downstream hyperpolarizing pathways in mesenteric arteries from spontaneously hypertensive rats. *Br J Pharmacology* 2010; 160: 836–843.
45. Tajada S, Cidad P, Moreno-Dominguez A, et al. High blood pressure associates with the remodeling of inward rectifier K^+ channels in mice mesenteric vascular smooth muscle cells. *J Physiol* 2012; 590: 6075–6091.
46. Zhang H, He C, Yan X, et al. Activation of inwardly rectifying K^+ channels by distinct PtdIns (4,5)P2 interactions. *Nat Cell Biol* 1999; 1: 183–188.